COMMINGLED YARNS OF SURFACE NANOSTRUCTURED FILAMENTS FOR EFFECTIVE COMPOSITE PROPERTIES

Edith Mäder, Christina Scheffler, Shang-Lin Gao, Julius Rausch
[Edith Mäder emaeder@ipfdd.de] Leibniz Institute of Polymer Research Dresden

Keywords: *commingled yarns; composites; sizing; interface; adhesion; nano-structuring*

Abstract

The online spinning process of commingled yarns is investigated in terms of distribution homogeneity and thermal shrinkage. In comparison with previous hybrid yarns intermingled by air jet texturing technology, the online spinning process could avoid fibre damage and improved the yarn distribution homogeneity. Our experiments show that both hybrid yarn tensile strengths and mechanical properties of unidirectional composites were improved based on an optimized sizing for glass fibres consisting of aminosilane and maleic anhydride grafted polypropylene film former. We found that the online commingled yarns do not tend to thermal shrinkage, whereas air jet textured yarns show shrinkage depending on the molecular orientation during processing of hybrid yarns or textile fabrics made thereof. Nanostructured interfaces introduced by smallest amounts of carbon nanotubes in sizings enable to achieve multifunctional effects such as improved tensile strength of glass fibres, modified morphology of interphases, and new fracture mechanisms.

1 Introduction

The hybrid yarn technology is a cost-effective processing method for continuous fibre thermoplastic composites, such as light weight components for vehicles. It could address a number of challenging issues of thermoset composites, including storage, long processing cycles, and high brittleness. Previous research on commingled yarns was mainly focussed on the air-jet texturing process. Because of the very short flow paths of the viscous polypropylene (PP) melt, commingled yarns offer an ideal opportunity to achieve short cycle times at improved homogeneity of impregnation. Both investigations in theoretical and experimental directions have been undertaken to utilize the high potential of light weight construction and the wide possibilities to design continuous-fibre reinforced composites with thermoplastic matrices [1-3]. A number of studies has been directed towards manufacturing of commingled yarn [1-5], properties of composites made from commingled yarn and effects of processsing conditions on impregnation, and consolidation behaviour [6-18].

The use of the textile reinforced thermoplastic composites in high performance light weight structural parts offers advantages compared to conventional constructions, particularly, in complex light weight applications and the function-integrating multi-material design. However, it was reported that the mechanical properties of the composites are strongly influenced by the hybrid yarn impregnation homogeneity, the unidirectional/textile subassemblies, the sizing on the glass fibre (GF), and the consolidation processing conditions. The effects of hydrothermal aging on commingled yarn GF/PP composites have been investigated [19]. It has been observed that an aminosilane sizing protects fibre against water, resulting in a diminution of the amount of absorbed water, where the interfacial interactions act as barriers during absorption and desorption. The extension and the profile of the Young's modulus of the interface between GF and PP matrix, because of interdiffusion and different chemical interactions, has been experimentally determined using Atomic Force Microscopy (AFM) [20]. Previous research on commingled yarns was mainly focussed on the air-jet texturing process. The literature contains few data about glass fibre/thermoplastic composites made from online hybrid yarns by simultaneous spinning and commingling of GF and

PP filaments. Presently, considerable efforts are undertaken to investigate the fracture behaviour of the commingled yarn composites. It is well known that intralaminar and interlaminar stresses result in relatively weak interlaminar fracture toughness, often leading to interlaminar failures such as delamination in composites under various loading conditions. In order to engage these challenges, researchers have developed 3D braided fibres as well as through-thickness stitching. A detailed review of these studies was given by Tong et al. [21]. However, these approaches do not account for all issues, such as low in-plane strengths for the 3D braided fibres and shorter tensile fatigue life and lower compression strengths for the stitched fibre laminates. Recently, carbon-nanotube reinforced polymer composites have reported limited improvements in the bulk mechanical properties compared with traditional fibre-reinforced composites. An effective utilization of nanotube mechanical potential in composites is a long standing problem, despite huge promise, issues such as dispersion, alignment, and interfacial strength still pose multiple challenges for the researches [22]. Extensive research efforts are required on the processing behaviour, the mechanical analysis of short and long term behaviour, and on the reliability models for dimensioning.

This paper deals with the equipment construction of online spinning of hybrid yarns, and with the investigation of material properties of online commingled yarn composites in comparison with those intermingled by air-jet texturing based on our previous work. We study the influence of different sizings and processing conditions on mechanical properties of the hybrid yarns, since the mechanical properties of composites can vary depending on the interphase between glass fibre (GF) and bulk matrix. To identify the tailored fibre and composite properties, we also investigated the distribution homogeneity of the polymer and reinforcement component, the thermal shrinkage and shrinkage stress behaviour, and the melt and crystallization. Further modification of fibre and interface properties has been achieved by incorporation of both single-walled carbon nanotubes (SWCNTs) and differently functionalized multi-walled carbon nanotubes (MWCNTs) into the sizing of glass fibres.

2 Experimental

2.1 Materials

The *commingled yarns* are made by separate spinning of E-glass fibre (GF) and polypropylene (PP) filaments with different sizings/finishs, which in turn are intermingled by air-texturing process, as described elsewhere [12]. The spinning speeds for this separate spinning were 1000 m/min for GF and 3000 m/min for PP, respectively. Furthermore, a commercial as received PP (Prolen-H, Chemosvit Fibrochem a. s., Slovakia) was used for comparison with self-made air-textured hybrid yarns. Two kinds of PP filaments were produced from either a commercial homopolymer (Borealis HH 450B) or a maleic anhydride modified polypropylene (MFR = 36 g/10 min) which was produced from isotactic homopolymer with the average molecular weight $M_w = 16\times10^4$ g/mol by blending with maleic anhydride grafted PP (Exxelor P1020 with $M_w = 8.6\times10^4$ g/mol). To perform pull-out tests with single-fibre composites the high molecular weight homopolymer ($M_w = 29\times10^4$ g/mol, Borealis HD 120M), also blended with maleic anhydride grafted PP (Exxelor P1020 with $M_w = 8.6\times10^4$ g/mol), was used as polymer matrix to investigate the most difficult conditions of alignment for the SWCNTs due to the high melt viscosity of the polymer matrix (MFR = 8 g/10 min).

To achieve best *interfacial interaction* for enhanced composite properties, we used standard commercial finishes and our PP-compatible sizings, namely *S* and *G*, respectively. As standard comercial finish, *S* Fasavin HT11 (Zschimmer & Schwarz) was applied to the polypropylene filaments. The specially developed sizing *G* consisted of Aminopropyltriethoxysilane AMEO (Degussa) and a nanodispersed polypropylene film former grafted with maleic anhydride having an average particle size distribution of 90 to 100 nm and a molecular weight of $M_w = 9.4\times10^4$ g/mol. The sizing formulation was prepared by slow stirring the AMEO in 50 % of the distilled water and further 30 min stirring to complete hydrolysis. The film former dispersion was diluted with distilled water and added to the silane solution. We explored different routes and stages to apply the sizing/finish on the both GF and PP fibres during the intermingling. Best results could be obtained for the case where no finish was applied to the PP-filaments and low amounts of sizing were applied to the GF (Fig. 1). Additionally, during the continuous spinning process, the GF were in-situ sized by the above described aqueous sizing *G* containing additional amounts of carbon nanotubes 0.04, 0.1, 0,2 wt% related to the sizing. The SWCNTs and MWCNTs were purchased from Nanocyl S.A., Belgium.

Fig. 1. Pilot plant equipment for online commingled yarn spinning of GF and PP. The insert shows the intermingling of GF (perpendicular) and PP (from right hand side)

The online hybrid yarns are made by *simultaneous spinning and commingling* of GF and PP filaments at a speed of approximately 700 m/min with fibre volume fraction of 50 % and a fineness of about 160 tex. We comprised the spatial integration of a thermoplastic melt spinning equipment into the workspace of the existing unique equipment for processing continuous GF filaments (Fig. 1) [24]. The optimised processing condition for a homogeneous mix of the GF and PP filament arrays has been established after comparing different technological routes including the adaption of the spinning velocity and the use of applicable nozzles for the PP spinning. The melt temperatures of GF and PP are 1200°C and 240°C, respectively. The cooling behaviour of the filaments, controlled by the processing speed, is crucial to determine the fibre diameter and in turn the constructive design of the filament haul-off, as well as the commingling and the winding process. Besides the circular cross sections of GF with diameters, D_f, of 12 to 24 µm, the PP filament diameter, D_m, is varied in the region of 12 to 45 µm according to processing conditions.

The *unidirectional composites* made of commingled yarns were processed in computer controlled long-term cycle (heating, consolidation, and cooling in the mould) at a temperature of 225°C for 45 min. In detail, heating from ambient temperature to 225°C took 23 min at a pressure of 0.5 MPa, followed by hot pressing at 3 MPa for 2 min and cooling down to 40°C for 20 min was applied. During cooling the pressure was kept constant at 3 MPa. To investigate the interfacial adhesion between the GF fibre and PP matrix, micro composites were prepared for the single fibre pull-out test. The single fibre was accurately embedded in the matrix (Borealis HD 120M with 2% Exxelor P1020) with embedding lengths of 800 µm.

2.2. Characterisation

The *distribution homogeneity* of reinforcement and matrix components of the hybrid yarns was analyzed with an optical microscope (OM) using polished cross sections of hybrid yarns embedded in epoxy resin. The samples were embedded in the resin and subsequently polished to obtain cross sections amenable to quantitative evaluation of the distribution homogeneity. In order to judge an representative amount of data four and five cross sections of air jet textured and online commingled yarns, respectively were evaluated. Because of partly scattered yarns, each cross section was divided into several areas, equal of width and breadth. The amount of areas used for the specific cross section partly differed due to sample preparation, but in any case the entirety of the used areas comprised all filaments throughout the cross section. After splitting up the cross section into several fragments, the area fraction of GF and PP was determined measuring every single filament within the relevant area by using the image analysis software analySIS. As a minimum, the evaluation of each cross section comprised 600 measured fibres and 10 sections. The weighted average relative frequency provides information on the distribution homogeneity of the examined hybrid yarns.

The *thermal shrinkage* behaviour was measured with a TST 2 by Lenzing Instruments, Austria. The instrument allows to record simultaneously the thermal shrinkage and the shrinkage force, both determined at a defined temperature and with a certain initial load. In preliminary measurements an initial load of 0,06 cN/tex was found to be a suitable value to provide the necessary pre-stressing of the hybrid yarn without dominating the small material

response due to shrinkage after going suddenly from room temperature to 165°C.

Atomic force microscopy (AFM, Digital Instruments D3100, USA) is used to determine the changes of the surfaces roughness of GF and PP fibres due to the different surface modification [20]. The topography of samples was studied in tapping mode. The phase images reveal differences in surface properties of the material which are currently only qualitative in nature and were produced using the following settings: a setpoint voltage equal to 50~55% of the free vibrational amplitude within a range from 2.0~2.5 V and integral and proportional gains of 0.2 and 2.0, respectively. The difference between the setpoint and the free amplitude is directly related to the force applied to the surface during imaging.

The *differential scanning calorimetry* (DSC) measurements were performed using a DSC7 (Perkin Elmer, USA) equipped with the Pyris-software in a temperature range from –60°C to 210°C. The temperature and heat of transition were calibrated with In and Pb standards. The heating rate used was always 20 K/min and the molten state at 210 °C was kept every time for 5 min to account for the thermal history and destroy in that way the pre-existing crystalline nuclei.

2.3. Mechanical testing

The tensile strength of single GF was measured using the Fafegraph Mechanical testing device (Fa. Textechno) equipped with a 100 cN force cell. The gauge length is 20 mm and the velocity is 10 mm/min under 65 % relative humidity and 20°C according to specification EN ISO 5079. Based on a vibration approach, the diameter of each selected fibre, D_f, was determined using a Vibromat ME (Fa. Textechno) according to specification EN ISO 53812 and ASTM D 1577. To verify the effect of surface properties on the statistical distribution of fibre tensile strength, the failure probabilities were fitted through the least squares method by single two-parameter Weibull model [25] using

$$P = 1 - \exp[-(\frac{\sigma}{s_0})^{m_0}] \qquad (1)$$

where P is the cumulative probability of failure (i/(n+1)) at the tensile stress σ. The parameters m_o and s_o are the Weibull modulus and the scale factor of fractured fibres, respectively.

The single fibre pull-out test was carried out on a self-made pull-out apparatus with force accuracy of 1 mN and displacement accuracy of 0.07 µm with identical pull-out velocities (0.01 µm/s) at ambient temperature. From each force–displacement curve, the force at start of debonding, F_d, the maximum force F_{max}, and the embedded length l_e were derived. The fibre diameter D_f of each pulled-out fibre was measured with an optical microscope. Every GF/PP combination was evaluated by about fifteen single tests. The apparent adhesion strength τ and the critical interphase energy release rate, G_{ic} were calculated, according to

$$\tau = F_{\max} / \pi D_f l_e \qquad (2)$$

$$F_d = \pi (D_f / 2)^2 \left(- p + \sqrt{p^2 - q(G_{ic})} \right) \qquad (3)$$

where p and $q(G_{ic})$ are terms depending on fibre and matrix mechanical properties and specimen geometry; their expressions and the derivation are given in [26], based on the theory originally presented in [27].

The transverse tensile strength σ_t is measured according to specification ISO 527 with a velocity of 1 mm/min (specimen dimensions of 4×15×140 mm). The intralaminar shear strength τ_c of samples (10×10×4 mm) is measured by a self-made compression shear test equipment with a deformation velocity of 1 mm/min.

3 Results and discussion

3.1 Distribution homogeneity

The performance of commingled hybrid yarns with high volume contents of reinforcement is intrinsically tied to the issue of distribution homogeneity of the components. Filament distribution homogeneity of online commingled and air jet textured hybrid yarns are compared. Fig. 2 shows a typical cross section of an online commingled hybrid yarn divided into various areas for subsequent evaluation.

Regardless the processing route of hybrid yarns, the ideal distribution of every single GF adjacent to PP could not be achieved neither in the case of online commingling nor air jet texturing. In any case the examined cross sections reveal agglomerates of either GF or PP filaments, but the size of these agglomerates differs significantly with regard to the chosen processing route. The hybrid yarns were determined to have a glass weight fraction of 75 wt%, equal to approximately 50 vol%. Based on these figures the aforementioned ideal state of distribution should result in an area fraction of 50 % GF for each evaluated cross section.

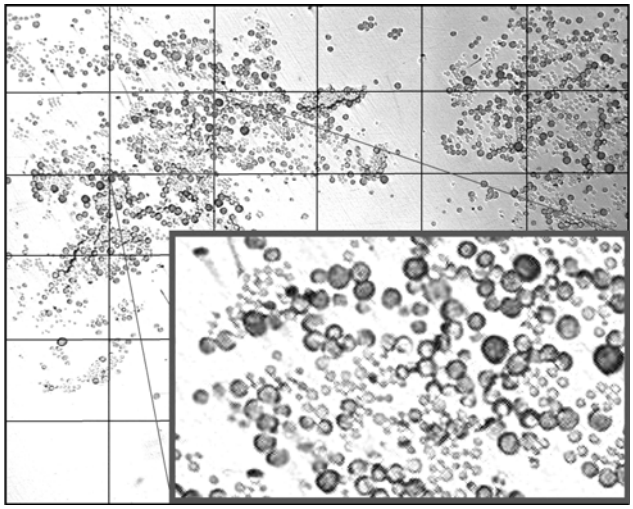

Fig. 2. Polished hybrid yarn cross section, sectioned for glass area fraction determination

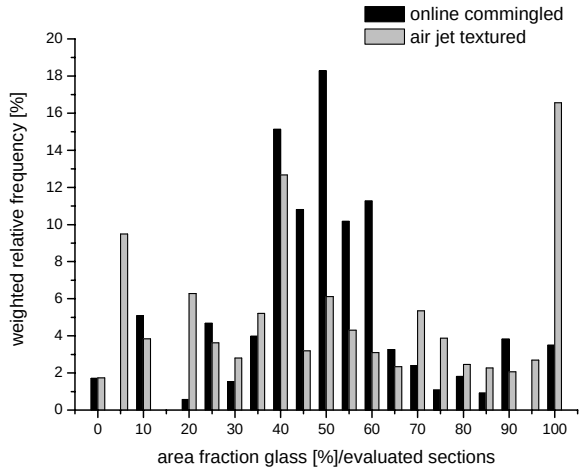

Fig. 3. Comparison between the distribution homogeneity of air jet textured and online commingled hybrid yarn

In Fig. 3 the averaged values for all examined hybrid yarns manufactured by either air jet texturing process or online commingling are shown and compared directly to each other. At first glance, both air jet textured and online commingled hybrid yarns show sections with unfavourable area fractions of glass being significantly different from the desired GF area fraction of 50%. For the online commingled yarns a distinct maximum of the relative weighted frequency around 50 % can be found and the outlying GF area fractions contain relatively few filaments, whereas the distribution homogeneity of the air jet textured yarns exhibits a comparably rugged shape. The limitations of the air jet texturing process for achieving good intermingling of the components became evident as the highest value for the weighted relative frequency is found to be at 100 %. In terms of distribution homogeneity of the yarn this can be interpreted as bundled GF agglomerates of significant dimensions.

Independent of the chosen commingling technique the results of the evaluated cross sections demonstrate the necessity of further improvement of intermingling, leading to an improved distribution with every GF being next to a PP filament. An optimised arrangement of the filaments would allow for shorter hot pressing cycles of the composite and thus further facilitate cost-efficient manufacturing.

3.2 Thermal shrinkage

Before hot pressing, the hybrid yarns usually undergo a preheating step where the thermoplastic filaments are molten to shorten cycle times. During this preheating process the flow-imposed molecular orientation of PP filaments tends to vanish and with increasing mobilization of the chains the thermodynamically beneficial random-coil state is approached. These mechanisms on the molecular level are associated with a macroscopically measurable shrinkage of the textile. As soon as the textile structures become more complicated, the inhomogeneous structure of the textile will result in a hardly predictable shrinkage behaviour and distortions of the textile which finally complicate the subsequent hot pressing process.

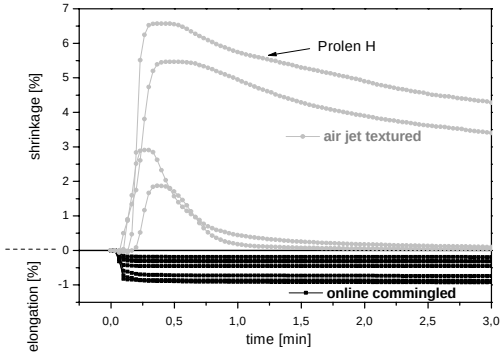

Fig. 4. Shrinkage/elongation as a function of time of air jet textured and online commingled yarns measured at a temperature of 165°C

Fig. 4 shows the recorded shrinkage behaviour for selected online commingled yarns in comparison with air textured yarns. Each curve represents the average of at least five measurements. The displayed curves comprise an representative selection of online and air textured yarns, including the air textured yarn based on commercially available Prolen-H filaments, showing interestingly the highest shrinkage among the air textured yarns. Depending on the type of hybrid yarn, two distinct regimes can be observed. The air jet textured yarns show an immediate response with the shrinkage shooting off and leading to a pronounced maximum in a plateau-like region within approximately 30 sec. Afterwards the measured shrinkage drops gradually, for two cases already reaching zero shrinkage within the measuring time. A totally opposed response is exhibited by the online commingled hybrid yarns. After starting the measurement, the hybrid yarns slightly elongate before the curves level off. Distinct local maxima like for the air jet textured yarns cannot be observed. The little increase in length can be attributed to the applied initial load being constant throughout measuring time and thus affecting the recorded elongation. Figure 4 demonstrates that the online commingled yarns do not tend to shrink at any time, thus, they are gradually pulled apart by the applied load until GF are fully stretched and further elongation is impeded. An explanation for the described behaviour of the two hybrid yarn types can be derived from the corresponding shrinkage stress vs. time curves in Fig. 5.

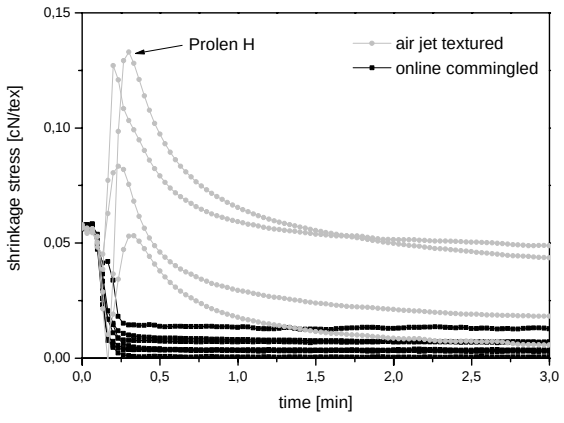

Fig. 5. Shrinkage stress as a function of time of air jet textured and online commingled yarns determined at a temperature of 165°C

All curves start off from the adjusted initial stress of 0,06 cN/tex. For the air textured yarns the recorded shrinkage stress rises quickly until it reaches a distinct maximum before falling off and stress relaxation phenomena take over. For the online commingled yarns at no time an increase in shrinkage stress can be recorded. The comparison of the general thermal shrinkage behaviour points out clearly the differences between the two hybrid yarn types.

During the shrinkage process mainly two forces contribute to the shrinkage process as becomes evident by Fig. 5: Before starting the measurements the only acting force is the initial load that generates a certain stress level in the clamped yarn. As soon as the temperature is applied the stress relaxation starts. In the case of the air jet textured yarns only a few seconds later the shrinkage stress builds up quickly acting in the opposed direction causing measurable shrinkage of the yarns. At the beginning of the measurement the shrinkage stress build-up is significantly faster than the stress relaxation mechanism taking place at the same time, however, the shrinkage stress ceases to affect the course of the measurement after approximately 30 seconds and again the stress relaxes gradually. The fact of the air textured yarns being proved to be more shrinkage-prone is attributed to the following reasons. Firstly, the PPs used for air jet texturing are spun at velocities causing a pronounced molecular orientation which is necessary to increase the strength level for textile manufacturing. Secondly, by air jet texturing a certain amount of GF is broken thus lowering their reinforcing effect and contribution to the yarn integrity, whereas in the case of online commingled yarns no filament damage occurs and lower take up velocities are used resulting in partly orientated yarns (POY).

3.4. Yarn and composite properties in dependence of the polymer/surface modification

Fig. 6 displays the yarn tensile strengths of online COM and two different air textured COM yarns. The online COM and air textured hybrid yarns compared contain the same sizing G, but no finish on the PP-filaments. Furthermore, the PP-matrix and modification is kept constant. The ratios D_m/D_f (in µm) are 24/17 for online COM and 12/12 for air textured yarns, respectively. The fibre volume content is kept constant at 50%. In comparison, the commercial PP-filaments used are unknown in both polymer and finish. Clearly, the air textured yarns show a significant decay of the tensile strength, which is due to damage of glass filaments caused by the high air pressure during intermingling. The two air textured yarns show a variation of the tensile strength which might be due to the different strand

integrity introduced by sizings/finishs. Similarly, we observed a remarkable improvement in mechanical properties of the composites made by the online hybrid yarns (Fig. 6b), although the diameters of the filaments are greater than those of the air-textured yarns. Particularly in transverse tensile strength a 30 % increase was achieved, which is attributed to better impregnation homogeneity and different interfacial states, as being introduced by the unknown commercial PP and finish on it. The air textured yarns possess somewhat reduced Young's modulus values induced by disorientations of reinforcement filaments.

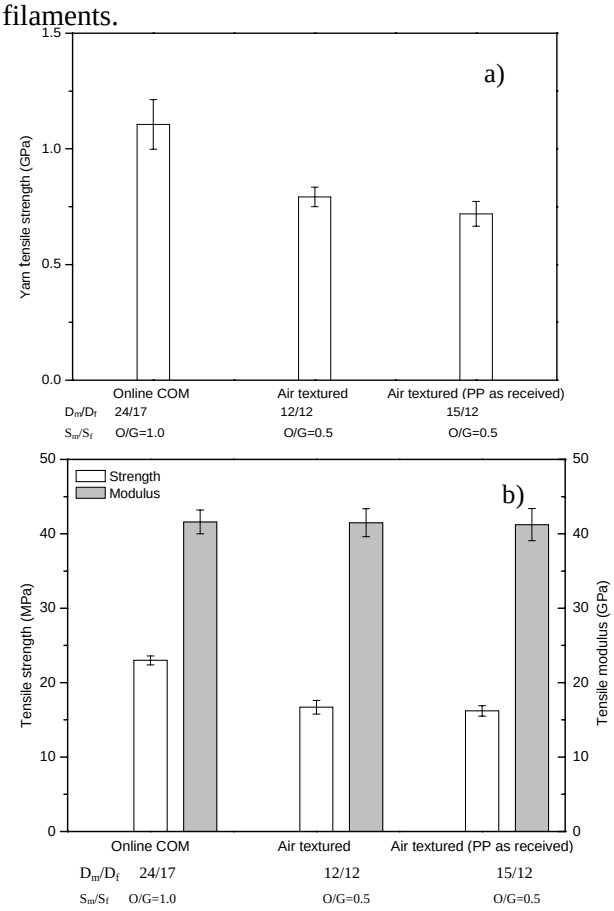

Fig. 6. Yarn tensile strengths (a), transverse tensile strengths and Young's moduli 0° of unidirectional composites (b, fibre volume fraction of 50 %) of online commingled and air textured yarns with diameters of matrix and reinforcement filaments (D_m/D_f, µm) and surface modification (S_m/S_f, wt%) (G glass sizing, O no finish). Error bars represent standard deviations

We further investigated in detail the mechanical properties of unidirectional composite plates made of commingled yarns with different PP and surface modifications. It shows that the use of modified PP leads to significantly increased transverse tensile strengths (about 23 MPa) compared to homo-PP (about 6 MPa). In comparison with unfinished PP-filaments the standard finish used for homo-PP filaments deteriorates the transverse tensile strength only marginally, e.g. variations in diameter ratios D_m/D_f from 12/12 up to 24/17 and surface modifications S_m/S_f: O/G revealed transverse tensile strengths variations between 18 and 24 MPa [30]. However, the huge difference is due to the presence and absence of covalent bonds for PPM and homo-PP, respectively.

It is well known that unidirectional fibre reinforced composites have a very low transverse tensile strength. This strength is normally lower than the strength of the pure matrix and limits the performance of the composite system. Assuming a perfect interfacial adhesion in the laminates, the transverse tensile strength, σ_t, can be estimated from [28]

$$\sigma_t = \left[1-(\sqrt{V_f}-V_f)(1-\frac{E_f V_m + E_m V_f}{E_f})\right]\sigma_m \qquad (4)$$

where σ_m is the matrix tensile strength. *V* and *E* are volume fraction and Young's modulus of the materials and the subscripts *f* and *m* refer to the properties of the fibre and the matrix, respectively. Taking E_f = 72 GPa, E_m = 1.2 GPa, σ_m = 30 MPa for E-glass fibre and PP, respectively, we can calculate σ_t to be ≈ 26.9 MPa, which is a fairly good agreement with experimentally determined values of the composites with the modified PP matrix, while it is much higher than that of the composites with the homo-PP associated with poor interfacial adhesion. This indicates a predominant effect of the interfacial adhesion properties on transverse tensile properties of laminated composites. It is evidenced that the enhancement of the adhesion by acid-base interactions or covalent bonds is possible only by the functionalisation of the PP combined with effective sizing on GF.

3.5. Nano-structured surfaces of online commingled yarns and model composites

SWCNTs or differently functionalized MWCNTs were concentrated in the interface by applying surface sizings with 0.04 wt% nanotubes related to the sizing or 6.7×10^{-4} wt% related to the PPM-matrix of the composite. In detail, we present results for the sizing G applied to GF and PPM-filaments with diameters of (D_m/D_f (µm): 17/17, sizings of S_m/S_f (wt%): O/G=1.0), and added 0.04 wt% SWCNTs related to the sizing. During online commingling the nano-structured surfaces are made simultaneously on GF and PP filaments. In the nano-

dispersed sizing we could reveal SWCNTs in AFM phase images of GF [30]. Although the concentration of CNT is very small, a positive effect on glass fibre tensile strength was observed. Interestingly, the average strain of the GF with SWCNTs increased by 10 %. As shown in Fig.7, both the Weibull plot lines and Weibull modulus, m_o, of nanotube coated systems shift to higher values corresponding to healing of surface flaws, which implies that the strength-controlling surface defects have lower heterogeneity of distribution and the size of defects is reduced [22]. In other words, the healed flaws on the fibres with SWCNTs show similar flaw size, severity and homogeneity relative to those without SWCNTs.

The interfacial parameters in GF/PP systems were characterised by single fibre pull-out tests. The data indicates a local adhesion strength of 30.2 MPa with SWCNTs compared with 22.1 MPa for the same GF/PP/sizing system without SWCNTs. The critical interface energy release rates determined are 31.8 and 14.0 J/m^2, correspondingly. The significant improvement of adhesion strength seems to be caused by a different failure mechanism (local interfacial bonding and crack bridging). Due to the mechanical interlinking with SWCNTs the roughness of the fracture surfaces is increased (Fig. 8 a,b) and the phase image (Fig. 8c) shows material inhomogeneity possibly caused by carbon nanotubes. Overall, the in-situ commingling process technology and nano-structured coatings show promising potential in cost-effective processing continuous fibre thermoplastic composites for different applications.

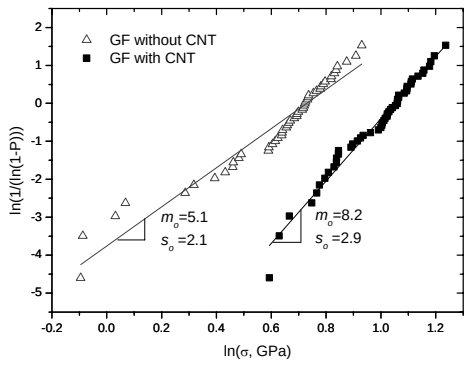

Fig. 7. Weibull plots of fibre fracture probability for GF with/without SWCNTs in the sizing

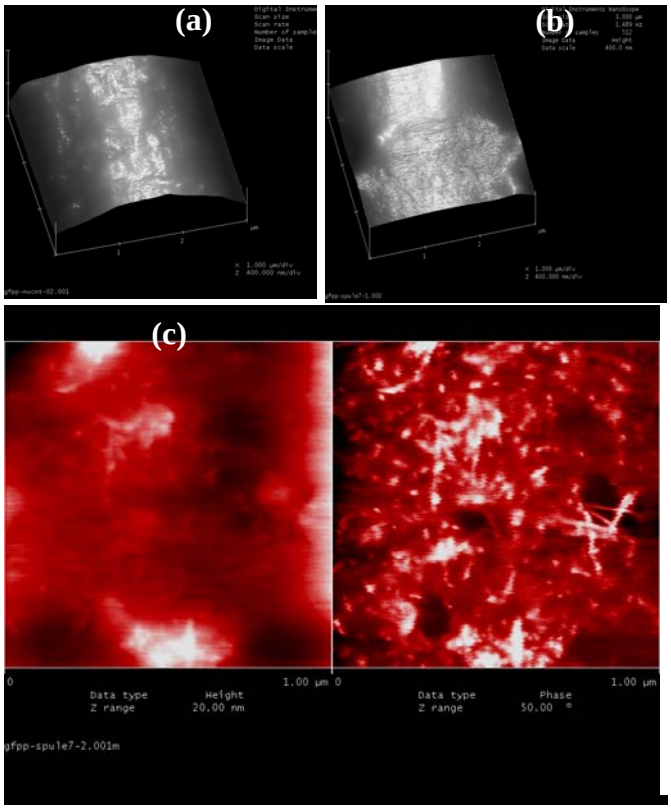

Fig. 8. AFM topography images of fracture surfaces of (a) GF without SWCNTs and (b) GF with SWCNTs in sizing after fibre pull-out test (x, y =3 µm, z = 400 nm). (c) AFM topography and phase images of GF with SWCNTs in sizing (x, y =1 µm, z = 20 nm, 50 °)

3.6 Crystallisation behaviour

In order to further investigate the impact of the carbon nanotubes on the crystallisation of the PP matrix, DSC measurements were carried out. Fig. 9 shows the heat flow for isothermal crystallisation at 140°C of online commingled yarn containing various amounts of MWCNTs. To account for the slightly varying amount of glass fibres within the samples, the displayed heat flow refers to the PP mass fraction of the samples, determined by subsequent pyrolysis of the hybrid yarns. As it was already reported in several studies [31-33], it is not surprising to find accelerated crystallisation kinetics for the samples containing a certain amount of MWCNTs, however, the applied weight fractions in this study are several orders of magnitude lower than it is usually the case for the nanocomposite materials. Compared to the reference case for the sizing without MWCNTs, the other hybrid yarns with MWCNTs show an accelerated crystallisation behaviour, where the onset of crystallisation as well as the point of maximum heat flow are shifted to notably smaller times. However, the content of

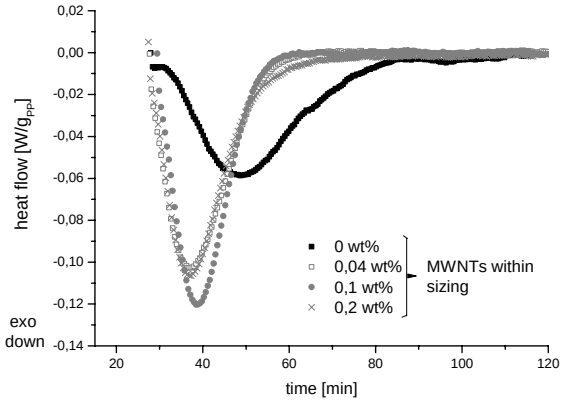

Fig. 9. Isothermal crystallisation at 140°C of online commingled yarns containing various amounts of MWCNTs

MWCNTs in the sizing does not affect notably the crystallisation kinetics, suggesting that a saturation of nucleation density is already reached for the low weight fractions applied to the sizings. An evaluation of the heating step after the isothermal crystallisation revealed increased enthalpies for the samples containing MWCNTs: Whereas for the reference sample a melt enthalpy of 124.7 J/g_{PP} was found, the samples with 0.04, 0.1, and 0.2 wt% MWCNTs within the sizing showed 129.46, 133.2, and 128.99 J/g_{PP}, respectively, thus providing evidence for the altered composite morphology in presence of the MWCNTs. Assuming the MWCNTs as spots for heterogeneous nucleation on the fibre surface, one can imagine that high nucleation density impedes the lateral growth of crystallites resulting in a transcrystalline layer around the GF. Light microscopy observation of the crystallisation using polarized light and a hot stage confirm these results (micrographs not shown). The existence of a transcrystalline layer around the GF fibre is known to be specific for the chosen fibre/sizing/matrix combination [34]. In the case of the used GF/PP system, the concentration of MWCNTs in the GF/PP interface by incorporating them into the GF-sizing provides an effective way to stimulate the growth of a transcrystalline layer.

4 Conclusions

Highlighting several processing relevant aspects of the commingling techniques, it could be shown that the online commingling technique offers various advantages over commingled hybrid yarns made by air jet texturing. Besides the glass filament damaging, inherent to the air texturing process and directly affecting the composite properties, also the distribution homogeneity was found to be improved and no thermal shrinkage could be observed for the online commingled yarns. The realization of minimized flow paths for the thermoplastic component associated with homogeneous filament distribution, thus, short hot pressing cycle time. We found that the online commingled yarns cause reduced thermal shrinkage. It facilitates the manufacturing of complex shaped textiles avoiding severe distortions during the pre-heating step, therefore, the thermal shrinkage appears to be one of major importance for the manufacturing of light weight structural parts based on hybrid yarns.

Regarding the surface modification of the fibres, promising first results could be obtained for the concentration of smallest amounts of SWCNTs in the interface. Those nanostructured interfaces involve multifunctional effects such as improved tensile strength, modified morphology of interphases, transcrystalline layers, and new fracture mechanisms.

Acknowledgements

This work was supported by the German Research Foundation (DFG) within the Collaborative Research Centre ‘Textile-reinforced composite components for function-integrating multi-material design in complex lightweight applications (SFB639)’. The authors are indebted to Dr. H. Brünig, B. Tändler and N. Smolka (spinning of PP), W. Ehrentraut, F. Eberth, R. Plonka (Spinning of GF), N. Schmidt and JW. Liu for technical assistance.

References

[1] Svensson N., Shishoo R., Gilchrist M. “Manufacturing of Composites from Commingled Yarns – A Review”. *J Thermopl Comp Mater* Vol.11, No. 1, pp. 22-56, 1998.

[2] Ruan XP., Chou TW. “Experimental and theoretical studies of the elastic behaviour of knitted-fabric composites”. *Comp Sci Technol* Vol. 56, No. 12, pp. 1391-1403, 1996.

[3] http://www.tu-dresden.de/mw/ilk/sfb639

[4] Wakeman MD., Cain TA., Rudd CD., Brooks R., Long AC. “Compression moulding of glass and polypropylene composites for optimised macro- and micro-mechanical properties – 1 Commingled glass and polypropylene”. *Comp Sci Technol* Vol. 58, No. 12, pp. 1879-1898, 1998.

[5] Alagirusamy R., Ogale V. “Commingled and Air Jet-textured Hybrid Yarns for Thermoplastic Composites”. *J Industr Textiles* Vol. 33, No. 4, pp. 223-243, 2004.

[6] Hamada H., Maekawa Z., Ikegawa N., Matsuo T., Yamane M. “Influence of the impregnating property on mechanical properties of commingled yarn composites”. *Polym Comp* Vol. 14, No. 4, pp. 308-313, 1993.

[7] Ye L., Friedrich K. "Mode I interlaminar fracture of co-mingled yarn based glass/polypropylene composites". *Comp Sci Technol* Vol. 46, No. 2, pp. 187-198, 1993.
[8] Ye L., Friedrich K. "Interlaminar fracture (mode II) of commingled yarn-based GF/PP composites". *J Mater Sci* Vol. 28, No. 3, pp. 773-7801993.
[9] Mäder E., Bunzel U., Schemme M. „Langfaserverstärkte Thermoplaste, Herstellung und Eigenschaften". *Technical Textiles* Vol. 37, No. 3, pp. T11-T14, 1994.
[10] Offermann P., Wulfhorst B., Mäder, E. „Hybridgarne für neuartige Verbundwerkstoffe aus Thermoplasten". *Technical Textiles* Vol. 38, No. 2, pp. 55-57, 1995.
[11] Shonaike GO., Hamada H., Maekawa Z., Matsuda M., Yuba T., Matsuo T. "The Influence of Cooling Conditions on the Mechanical Properties of Commingled Yarn Composites". *J Thermopl Comp Mater* Vol. 9, No. 1, pp. 76-89, 1996.
[12] Stumpf H., Mäder E., Baeten S., Pisanikovski T., Zäh W., Eng K., Andersson CH., Verpoest I., Schulte K. "New thermoplastic composite preforms based on split-film warp-knitting". *Comp Part A* Vol. 29, No. 12, pp. 1511-1523, 1998.
[13] Mäder E., Skop-Cardarella K. "Tailored Thermoplastic Composites Based on New Hybrid Yarns". *Key Eng Mater* Vol. 137, pp. 24-31, 1998.
[14] Bogoeva-Gaceva G., Mäder E., Queck H. "Properties of Glass Fiber Polypropylene Composites Produced from Split-Warp-Knit Textile Preforms". *J Thermopl Comp Mater* Vol. 13, No. 9, pp. 363-377, 2000.
[15] Long AC., Wilks CE., Rudd CD. "Experimental characterisation of the consolidation of a comingled glass/polypropylene composite". *Comp Sci Technol* Vol. 61, No. 11, pp. 1591-1603, 2001.
[16] Vendramini J., Bas C., Merle G., Boissonnat P., Alberola NP. "Commingled poly(butylene terephthalate)/unidirectional glass fiber composites: Influence of the process conditions on the microstructure of poly(butylene terephthalate)". *Polym Comp* Vol. 21, No. 5, pp. 724-733, 2000;
[17] Bernet N., Michaud V., Bourban PE., Månson JAE. "Commingled yarn composites for rapid processing of complex shapes". *Comp Part A* Vol. 32, No. 11, pp. 1613-1626, 2001.
[18] Putnoki I., Moos E., Karger-Kocsis J. "Mechanical performance of stretched knitted fabric glass fibre reinforced poly(ethylene terephthalate) composites produced from commingled yarn". *Plastics Rubber Composites* Vol. 28, No. 1, pp. 40-46, 1999.
[19] Lariviere D., Krawczak P., Tiberi C., Lucas P. "Hydrothermal aging of GF/PP composites: When glass/polymer adhesion favours water entrapment". *Polym and Polym Comp* Vol. 13, No. 1, pp. 27-35, 2005.
[20] Gao SL., Mäder E. "Characterisation of interphase nanoscale property variations in glass fibre reinforced polypropylene and epoxy resin composites". *Comp Part A* Vol. 33, No. 4, pp. 559-576, 2002.
[21] Tong L., Mouritz AP., Bannister M. "*3D Fibre Reinforced Composites*". Elsevier, Oxford, 2002.
[22] Gao SL., Mäder E., Plonka, R. "Nanostructured coatings of glass fibers: Improvement of alkali resistance and mechanical properties. *Acta Materialia* Vol. 55, No. 3, pp. 1043-1052, 2007.
[23] Report AiF-Nr. 322D (1993) Report AiF-Nr. 10039 B (1996) Report AiF-Nr. 11644B (2000), Leibniz-Institut für Polymerforschung Dresden.
[24] Online Hybridgarnspinnen von Glasfaser- und Thermoplastfilamenten. *Annual Report Leibniz-Institute for Polymer Research Dresden*, p. 64, 2005.
[25] Weibull W. "A statistical distribution function of wide applicability". *J. Appl. Mech. –Transactions of the ASME* Vol. 18, No. 3, pp. 293-297, 1951.
[26] Zhandarov S., Pisanova E., Mäder E. "Is there any contradiction between the stress and energy failure criteria in micromechanical tests? Part II. Crack propagation: Effect of friction on force-displacement curves. *Comp Interf* Vol. 7, No. 3, pp. 149-175, 2000.
[27] Nairn JA. "Analytical fracture mechanics analysis of the pull-out test including the effects of friction and thermal stresses". *Adv Comp Lett* Vol9, No. 6, pp. 373-383, 2000.
[28] Kaw AK. "*Mechanics of Composite Materials*". CRC Press, 2006.
[29] Mäder E., Rothe C., Liu JW. "Verbundwerkstoffe auf Basis von Hybridgarnen mit maßgeschneiderter Oberflächenmodifizierung. *Proc. of Technomer Conf.*, Chemnitz, Germany, 2005, p. 1-15.
[30] Mäder E., Rothe C., Gao S L. "Commingled yarns of surface nanostructured glass and polypropylene filaments for effective composite properties". *J Mater Sci*, in press.
[31] Valentini L., Biagiotti J., Lopez-Manchado M., Santucci S., Kenny J. "Effects of carbon nanotubes on the crystallization behavior of polypropylene". *Polymer Engineering and Science* Vol. 44, pp. 303-311, 2004.
[32] Grady B., Pompeo F., Shambough R., Resasco D. "Nucleation of polypropylene crystallization by SWCNT". *Journal of Physical Chemistry, Part B*, Vol. 106, pp.5852-5858, 2002.
[33] Seo M., Lee J., Park S. "Crystallization kinetics and interfacial behaviors of polypropylene composites reinforced with multi-walled carbon nanotubes". *Materials Science and Engineering* Vol. A404, pp. 79-84, 2005.
[34] Quan H., Li Z., Yang M., Huang R. "On transcrystallinity in semi-crystalline polymer composites". *Composites Science and Technology* Vol. 65, pp. 999-1021, 2005.